

CAD-Prompted SAM3: Geometry-Conditioned Instance Segmentation for Industrial Objects

Zhenran Tang, Rohan Nagabhirava, Changliu Liu

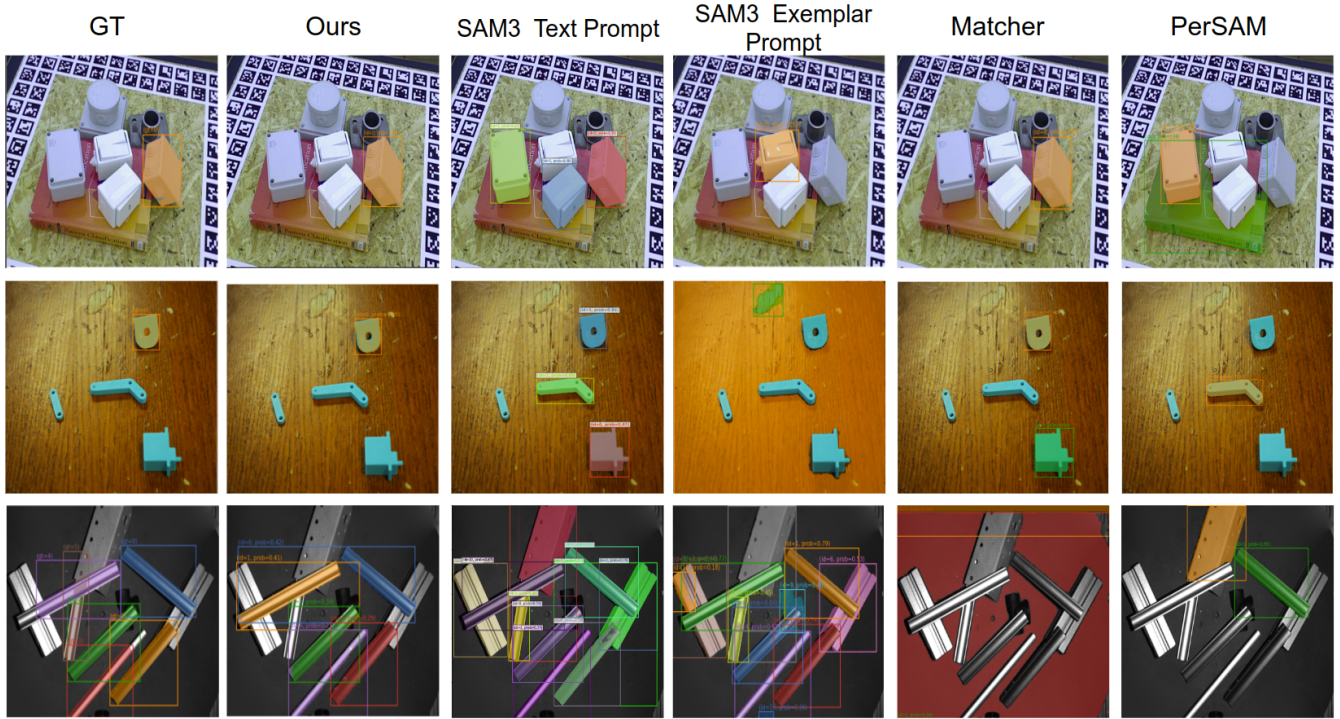


Fig. 1: Qualitative comparison of CAD-prompted SAM3 with SAM3 (exemplar and text prompts), Matcher, and PerSAM. Our approach produces more accurate instance masks given identical CAD-based prompts. Text prompts for SAM3 are generated from the CAD renderings using GPT-5.1.

Abstract—Verbal-prompted segmentation is inherently limited by the expressiveness of natural language and struggles with uncommon, instance-specific, or difficult-to-describe objects—scenarios frequently encountered in manufacturing and 3D printing environments. While image exemplars provide an alternative, they primarily encode appearance cues such as color and texture, which are often unrelated to a part’s geometric identity. In industrial settings, a single component may be produced in different materials, finishes, or colors, making appearance-based prompting unreliable. In contrast, such objects are typically defined by precise CAD models that

capture their canonical geometry.

We propose a CAD-prompted segmentation framework built on SAM3 that uses canonical multi-view renderings of a CAD model as prompt input. The rendered views provide geometry-based conditioning independent of surface appearance. The model is trained using synthetic data generated from mesh renderings in simulation under diverse viewpoints and scene contexts. Our approach enables single-stage, CAD-prompted mask prediction, extending promptable segmentation to objects that cannot be robustly described by language or appearance alone.

Zhenran Tang, Rohan Nagabhirava, and Changliu Liu are with the Robotics Institute, Carnegie Mellon University, Pittsburgh, PA, USA ({zhenrant, rnagabhi, cliu6}@andrew.cmu.edu). In collaboration with Lockheed Martin Advanced Technology Laboratories (LM ATL). Research was sponsored by the ARM (Advanced Robotics for Manufacturing) Institute through a grant from the Office of the Secretary of Defense and was accomplished under Agreement Number W911NF-17-3-0004. The views and conclusions contained in this document are those of the authors and should not be interpreted as representing the official policies, either expressed or implied, of the Office of the Secretary of Defense or the U.S. Government. The U.S. Government is authorized to reproduce and distribute reprints for Government purposes notwithstanding any copyright notation herein.

I. INTRODUCTION

Robotic manipulation in cluttered environments depends on reliable perception to identify target objects before planning interaction. Instance segmentation is commonly used to separate objects from background and neighboring items, producing masks that can be used to filter point clouds for pose estimation and grasp selection. Integrated systems in robotic competitions such as RoboCup@Home [1] and the Amazon Picking Challenge [2] include segmentation

as part of the perception pipeline for object localization and manipulation. In practice, YOLO-style models provide accurate and efficient detection and segmentation suitable for real-time robotic applications. However, achieving reliable performance on new object categories typically requires collecting and annotating hundreds of instances per class. In rapid prototyping and small-batch manufacturing settings, where new parts are introduced frequently and produced in small quantities, this data requirement can be a significant hurdle.

Recent advances in promptable segmentation, particularly foundation models such as the Segment Anything Model 3 (SAM3) [3], demonstrate strong generalization across open-world imagery and support both language and image-exemplar prompting. Language-prompted vision models perform well for broad semantic categories but are less suitable for engineered components, which often lack descriptive names and are distinguished by subtle geometric differences that vision language models have difficulty resolving [4], [5].

Image-exemplar prompting reduces linguistic ambiguity by conditioning on visual references. However, exemplar-based methods degrade when substantial intra-class appearance variation exists between support and query images [6]. In rapid prototyping and small-batch manufacturing, this is a significant limitation, as the same component may be produced in different colors, materials, or surface finishes.

In contrast, engineered objects are canonically defined by their CAD models. A CAD file specifies the exact geometry of a component independent of its surface appearance. In this work, we introduce a CAD-prompted segmentation framework that extends promptable segmentation to geometry-defined objects. Building upon SAM3, we use canonical multi-view renderings of a CAD model as prompt inputs to condition segmentation on geometric structure while remaining independent of surface appearance. The model is trained using large-scale synthetic data generated by rendering mesh-based objects with randomized color and textures, to enable instance segmentation for objects that are difficult to describe by language or exemplar images, as shown in Fig. 1. Our contributions are:

- We formulate CAD-prompted promptable segmentation, introducing canonical multi-view renderings as a geometry-aware prompt modality.
- We present a synthetic training pipeline that leverages mesh renderings to disentangle geometry from appearance variation.
- We demonstrate that CAD prompts enable robust single-stage dense mask prediction for industrial objects across varying materials and surface properties.

By conditioning segmentation on CAD-defined geometry rather than semantic labels or exemplar appearance, our framework aligns perception with how engineered components are specified in manufacturing practice. This enables reliable open-set instance segmentation for parts whose identity is determined by shape rather than color, texture, or language.

II. RELATED WORK

A. Foundation Segmentation Models

Foundation segmentation models replace fixed semantic classifiers with flexible input prompts such as points, boxes, language, or image exemplars. The original Segment Anything Model (SAM) introduced large-scale prompt-conditioned mask prediction and demonstrated strong generalization across datasets [7]. SAM3 further extends this framework to promptable concept segmentation, enabling mask prediction conditioned on text and image exemplars across images and videos [3]. These works show that segmentation can be formulated as a general prompt-conditioned task. However, when conditioned on visual exemplars, the representation remains based on appearance similarity.

B. Appearance-Based Exemplar Conditioning

Several works perform cross-image segmentation by conditioning on a visual exemplar. Earlier few-shot segmentation methods such as CANet and PFENet compute dense feature correspondences between support and query images, using the resulting similarity maps to guide subsequent mask prediction modules [8], [9]. Within the SAM framework, PerSAM computes similarity in SAM’s image embedding space to derive explicit point prompts, along with high-level semantic prompts and target-guided attention to improve mask prediction [10]. Matcher performs bi-directional feature matching using an external DINOv2 [11] backbone to generate point prompts, and then applies SAM for mask prediction [12]. Despite architectural differences, these methods rely primarily on explicit dense support–query feature similarity to guide segmentation.

C. CAD-Based Detection with Proposal Matching

Modern model-based, unseen object detection methods on RGB images typically generate object proposals and match them against rendered views of a predefined set of CAD models using pretrained visual features. Representative systems include CNOS, which first uses SAM [7] to segment all possible object instances as proposals, then scores proposals against CAD-rendered views using DINO [13] features to identify object instances [14]. Subsequent works such as MUSE [15] and NIDS-Net [16] improve this pipeline by adopting stronger proposal models and feature backbones, and refining similarity scoring. These approaches evaluate multiple object candidates per image and perform per-object scoring against a set of CAD models, rather than providing a unified promptable segmentation interface.

D. Geometry-Conditioned Prompting

Existing exemplar-based methods rely on support–query similarity maps to guide segmentation, while proposal-matching pipelines use CAD models only after mask generation, scoring object proposals against a predefined CAD model set within a two-stage detection framework. In contrast, we formulate CAD-prompted perception as a single-stage promptable segmentation problem. Built on

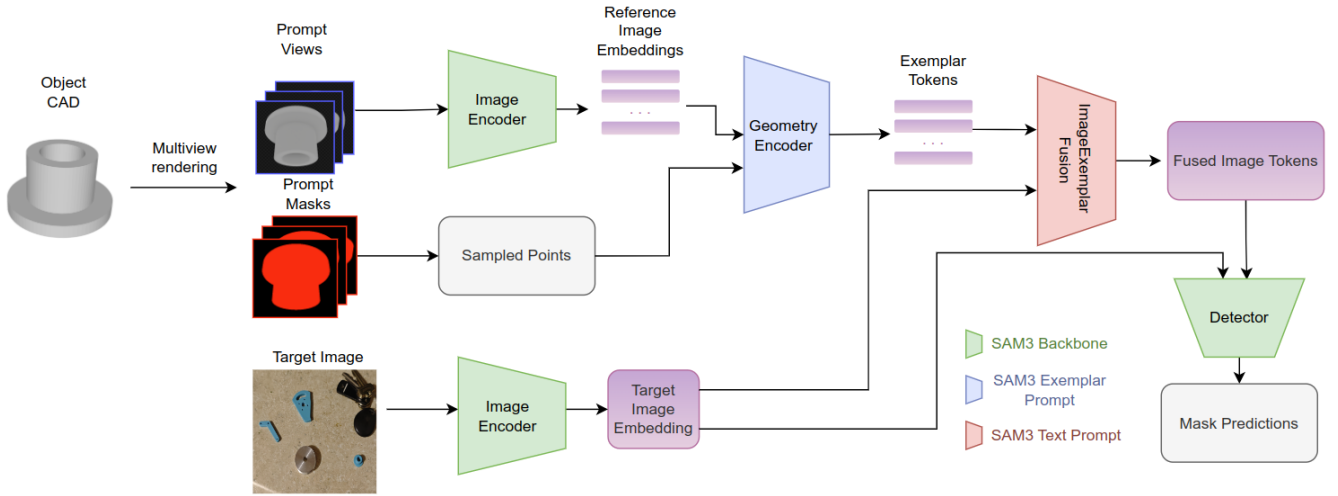


Fig. 2: Model architecture. Canonical multi-view renderings of a CAD mesh are encoded into geometry-aware embeddings, which are injected as cross-image prompt tokens into a fusion transformer. The fused features are processed by the SAM3 detection and mask heads to produce instance masks in one forward pass.

SAM3 [3], our method replaces RGB exemplars with canonical multi-view renderings of CAD models to allow geometry-conditioned mask predictions.

III. METHODOLOGY

We extend the SAM3 architecture to enable geometry-conditioned segmentation driven solely by CAD models. We first revisit the relevant components of SAM3, then define our CAD-prompted segmentation task, and finally introduce our geometry-based prompting mechanism and training procedure.

A. Revisiting SAM3

SAM3 is a promptable segmentation model that predicts instance masks conditioned on input prompts. It consists of four primary components:

- **Image Encoder:** extracts dense visual tokens from an input image.
- **Prompt Encoder:** converts prompts into embedding tokens, including `GeometryEncoder` for point prompts and `textEncoder` for text prompts.
- **Fusion Transformer:** conditions image features on prompt embeddings via cross-attention.
- **Detection Head and Mask Decoder:** predict instance tokens and decode them into pixel-level segmentation masks.

Given an image I , the image encoder produces visual tokens

$$T_I = \text{ImageEncoder}(I).$$

Given prompt embeddings E , the fusion transformer computes

$$T_{\text{fused}} = \text{FusionTransformer}(T_I, E),$$

which are subsequently processed by the detection head and mask decoder to produce instance masks.

SAM3 also supports exemplar prompting via the `GeometryEncoder`, which encodes point-conditioned features from the same input image and feeds them directly into the detection module. In the original formulation, exemplar prompts are assumed to originate from the query image itself.

In our work, we retain the image encoder, fusion transformer, detection head, and mask decoder of SAM3. Our contribution lies in extending the prompt interface to support geometry-conditioned embeddings derived from CAD models.

Task Definition: CAD-Prompted Segmentation

We consider the problem of segmenting all visible instances of a target object in a query RGB image given only its 3D mesh as specification.

Formally, given:

- A target mesh \mathcal{M} ,
- A query RGB image $I \in \mathbb{R}^{H \times W \times 3}$,

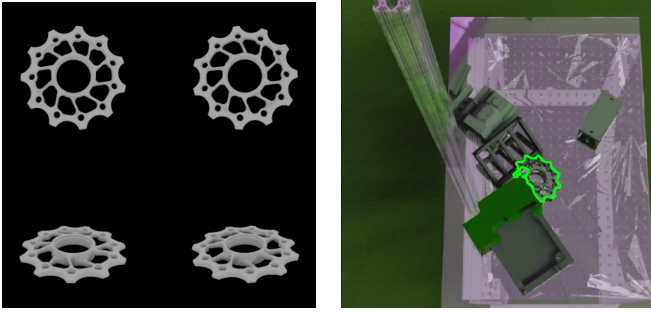
the goal is to predict binary masks $\{\hat{S}_k\}$ corresponding to all visible instances of \mathcal{M} in I .

No textual description, category label, or real image exemplar is provided at inference time. The only object specification is the 3D geometry \mathcal{M} . The objective is to condition dense mask prediction directly on geometric specification within a promptable segmentation framework.

B. Geometry-Conditioned Prompt Construction

In our setting, the exemplar is derived from rendered views of a CAD model and therefore originates from a different image domain than the query image. Directly feeding such cross-image exemplar embeddings into the detection head, as in the original same-image exemplar formulation, leads to weak alignment between prompt features and query image features.

To address this, we introduce a mesh-to-prompt conversion pipeline that explicitly re-aligns geometry-derived



(a) Multi-view CAD renderings as prompt. (b) Synthetic training scene with GT contour.

Fig. 3: Geometry-conditioned training pipeline. (a) Canonical CAD renderings serve as prompts. (b) Synthetic training data with instance annotations.

embeddings with the query image through the SAM3 fusion transformer.

a) Multi-View Mesh Rendering.: Given a CAD mesh \mathcal{M} , we render it from predefined canonical viewpoints $V = 12$ using Blender. The viewpoints are distributed over the viewing sphere to capture diverse geometric perspectives. Multi-view projections have been shown to provide an effective representation of 3D shape by encoding complementary geometric information across viewpoints [17]. Subsequent work demonstrated that modeling relationships across views further enhances geometric encoding quality [18]. Each rendering produces an RGB image R_v and its corresponding foreground mask (Fig. 3a).

b) View Encoding via Sequence Geometry Encoder.: Each rendered view R_v is encoded using the SAM3 image encoder:

$$T_v = \text{ImageEncoder}(R_v).$$

To emphasize geometric structure, we uniformly sample 25 point prompts within the foreground mask of each rendering. The image tokens T_v and the point prompts P_v are passed through the SAM3 `GeometryEncoder`:

$$E_v = \text{GeometryEncoder}(T_v, P_v).$$

This yields a set of geometry-aware exemplar embeddings $\{E_v\}_{v=1}^V$ representing canonical views of the mesh.

c) Cross-Image Prompt Fusion.: Unlike the same-image exemplar prompt in SAM3, we do not feed $\{E_v\}$ directly into the detection head. Instead, we reinterpret geometry-derived embeddings as concept tokens and route them through the SAM3 text-image fusion transformer.

Given query image tokens

$$T_I = \text{ImageEncoder}(I),$$

we compute

$$T_{\text{fused}} = \text{FusionTransformer}(T_I, \{E_v\}_{v=1}^V).$$

The transformer-based fusion module naturally supports a variable number of prompt tokens, allowing multiple viewpoint embeddings to be injected without architectural

modification. Self-attention within the transformer enables interaction among viewpoint tokens, allowing multi-view geometric information to be aggregated before conditioning the image features.

This fusion step is critical for aligning cross-image geometry embeddings with query image features and enables effective geometry-conditioned segmentation.

C. Single-Stage Detection and Segmentation

The fused representation T_{fused} is processed by the inherited SAM3 detection head to generate instance tokens. Each instance token D_k is decoded by the mask decoder to produce a segmentation mask:

$$\hat{S}_k = \text{MaskDecoder}(T_{\text{fused}}, D_k).$$

Detection and segmentation are performed in a single forward pass conditioned directly on the CAD-derived prompt.

D. Training with Synthetic Data

Although the backbone architecture is reused from SAM3, fine-tuning is required to align geometry-derived prompt embeddings with image features and to encourage geometry-focused reasoning.

a) Synthetic Dataset Generation.: We collect approximately 9,000 CAD models from the ABC Dataset[19]. Multi-object scenes are generated with Isaac Sim’s Replicator pipeline by placing meshes in cluttered environments under diverse lighting conditions and background textures (Fig. 3b). The pipeline employs Automated Domain Randomization (ADR) across 21 independently configurable parameters spanning PBR material assignment, HDR lighting profiles, camera intrinsics and extrinsics, object scale and pose variation, and distractor placement. This randomization is designed to simulate the diversity of real manufacturing environments, including varying surface finishes, lighting conditions, and scene clutter, to prevent the model from exploiting appearance shortcuts and encourage geometry-based reasoning from CAD priors. Pixel-level ground-truth masks are obtained automatically from simulation.

b) Appearance Randomization.: To reduce reliance on color and texture cues, object materials, colors, and surface properties are randomly assigned independently of mesh identity. This encourages invariance with manufacturing variations and promotes geometry-driven segmentation.

c) Optimization Objective.: Training is conducted in two stages to balance stability and multi-instance detection capability. Although DETR-style models often employ one-to-one matching to avoid post-processing, we found that strict one-to-one supervision leads to unstable optimization.

Stage 1: Score-Weighted Mask Supervision

In the initial stage, we supervise all predicted masks using a score-weighted mask loss. Each predicted instance includes a mask \hat{S}_k and a detection score s_k . For each prediction, we compute a mask loss consisting of binary cross-entropy (BCE) and Dice loss:

$$\mathcal{L}_{\text{mask}}^{(k)} = \mathcal{L}_{\text{BCE}}(\hat{S}_k, S_k^*) + \mathcal{L}_{\text{Dice}}(\hat{S}_k, S_k^*),$$

where S_k^* denotes the ground-truth mask that best matches the prediction \hat{S}_k , defined as

$$S_k^* = \arg \max_{S_j \in \mathcal{G}} \text{IoU}(\hat{S}_k, S_j),$$

where \mathcal{G} is the set of ground-truth instance masks in the image.

We weight each mask loss by its predicted detection score:

$$\mathcal{L}_{\text{stage1}} = \sum_k s_k \cdot \mathcal{L}_{\text{mask}}^{(k)}.$$

This formulation supervises all predicted outputs and provides strong gradient signals during early training, leading to improved optimization stability. However, since each prediction is independently encouraged to match any ground-truth mask without explicit instance-level assignment, this objective does not enforce coverage across distinct object instances. As a result, multiple predictions may collapse onto the same instance, while ignoring others when multiple instances are present.

Stage 2: One-to-Many Matching.

After the model learns basic geometric alignment between CAD prompts and image features, we switch to a one-to-many matching strategy to enable multi-instance prediction.

For each ground-truth instance, we allow up to $K = 5$ predictions to be matched based on IoU-based greedy matching. The loss consists of matched mask loss (BCE + Dice) for selected predictions and presence loss supervising detection scores:

$$\mathcal{L}_{\text{stage2}} = \sum_{k \in \mathcal{M}} \mathcal{L}_{\text{mask}}^{(k)} + \mathcal{L}_{\text{presence}},$$

where \mathcal{M} denotes the set of matched predictions. The presence loss supervises detection scores such that matched predictions are assigned a target label of 1, and unmatched predictions are assigned 0. Formally, for each prediction k , we define a binary target

$$y_k = \begin{cases} 1, & k \in \mathcal{M}, \\ 0, & \text{otherwise,} \end{cases}$$

and compute a binary cross-entropy loss on the detection score s_k :

$$\mathcal{L}_{\text{presence}} = \sum_k \mathcal{L}_{\text{BCE}}(s_k, y_k).$$

This objective encourages the model to cover multiple object instances rather than collapsing predictions onto a single instance. During inference, non-maximum suppression (NMS) is applied to remove redundant overlapping predictions.

E. Inference

At inference time, only the target mesh \mathcal{M} and the query image I are required. The mesh is rendered into canonical views, encoded into geometry-conditioned prompt embeddings, fused with image features, and decoded in a single forward pass to produce segmentation masks.

This formulation extends SAM3 from language-conditioned and same-image exemplar prompting to cross-image, CAD-conditioned segmentation while preserving its single-stage, promptable architecture.



Fig. 4: Representative samples from the custom 3D printing dataset.

IV. EXPERIMENTAL RESULTS

A. Experiment Setup

a) Evaluation Protocol. For all datasets, we adopt a prompt-based evaluation protocol. For each image, we issue one prompt per ground-truth object category present in that image. Each prompt is expected to segment all visible instances of the corresponding object within that image. This setup evaluates prompt-conditioned instance segmentation rather than closed-set detection over a predefined set of objects.

Since SAM3 does not originally support exemplar prompts from a different image domain, directly injecting cross-image prompt embeddings leads to degraded performance due to feature misalignment. To ensure fair comparison, we route exemplar features through the original ImageExemplarFusion module before mask prediction, following the same cross-image fusion mechanism used in our geometry-conditioned pipeline.

b) Metrics. We report Panoptic Quality (PQ) and instance-level F1 score. PQ jointly measures segmentation accuracy and instance recognition quality, while F1 evaluates instance-level detection performance based on mask overlap. Together, these metrics capture both dense mask precision and multi-instance prediction accuracy.

B. 3D Printing Dataset

To evaluate geometry-conditioned segmentation in rapid prototyping scenarios, we construct a custom dataset consisting of 8 distinct 3D-printed objects derived from CAD models. The dataset contains 80 real-world RGB images with an average of 3.5 object instances per image. Each object is printed in two different colors, and images are captured under diverse backgrounds with unrelated distractor objects (Fig. 4).

The 8 objects do not appear in the synthetic data used for training the model, ensuring evaluation on unseen geometries. Ground-truth instance masks are manually annotated for all objects.

Table I reports performance. Our method achieves the highest segmentation quality, obtaining a PQ of 0.7385 and an F1 score of 0.7636. Matcher achieves competitive performance (PQ 0.6057, F1 0.6271), while PerSAM and direct SAM3 exemplar prompting perform substantially worse. These results demonstrate that geometry-conditioned prompting provides a clear advantage in rapid prototyping settings where object identity is defined by shape rather than surface appearance.

TABLE I: Performance on the custom 3D printing dataset.

Method	PQ	F1
Matcher	0.6057	0.6271
PerSAM	0.2846	0.5035
SAM3 Image Exemplar Prompt	0.1713	0.1935
CAD-Prompted SAM3 (Ours)	0.7385	0.7636

TABLE II: Performance on T-LESS and ITODD benchmarks.

Method	T-LESS		ITODD	
	PQ	F1	PQ	F1
Matcher	0.2637	0.3050	0.2874	0.3520
PerSAM	0.1660	0.1880	0.2502	0.3621
SAM3 Image Exemplar Prompt	0.1710	0.1894	0.4152	0.5070
CAD-Prompted SAM3 (Ours)	0.2799	0.3329	0.4921	0.6090

C. Benchmark Datasets

We further evaluate on two standard industrial benchmarks: T-LESS[20] and ITODD[21]. All benchmark results are reported on the official test splits.

a) *T-LESS*.: T-LESS is an industry-related object dataset consisting of texture-less rigid components. The objects have no identifiable color or texture, many exhibit strong geometric similarity, and scenes are highly cluttered with significant occlusion. These characteristics make instance discrimination challenging for appearance-based methods.

b) *ITODD*.: ITODD is an industrial setting dataset featuring texture-less metallic objects captured in grayscale. The dataset includes both uncluttered and highly cluttered scenes, emphasizing shape-based reasoning under limited appearance cues.

Table II summarizes benchmark performance. On T-LESS, our method achieves the highest PQ (0.2799) and F1 (0.3329), outperforming all baselines. On ITODD, our approach yields a substantial improvement, reaching PQ 0.4921 and F1 0.6090. The consistent gains across both datasets indicate that conditioning segmentation directly on canonical CAD geometry improves robustness in industrial object perception.

V. CONCLUSION AND FUTURE WORK

A. Conclusion

We presented a geometry-conditioned promptable segmentation framework that extends foundation segmentation models to industrial objects defined by CAD specifications. Instead of relying on language descriptions or RGB exemplars, our method conditions segmentation directly on canonical multi-view renderings derived from CAD models, enabling shape-based object identification independent of surface appearance.

Built upon SAM3, our approach formulates CAD-conditioned perception as single-stage promptable instance segmentation. Across a custom 3D printing dataset and standard industrial benchmarks including T-LESS and ITODD, CAD-Prompted SAM3 consistently improves segmentation quality over appearance-based exemplar methods. The gains

are particularly pronounced in rapid prototyping scenarios where objects vary in color and context but retain fixed geometry.

These results demonstrate that canonical geometry can serve as a robust and expressive prompt modality for foundation segmentation models. By aligning perception with the way industrial objects are defined—through precise CAD models rather than textual labels or visual exemplars—our formulation offers a practical solution for perception for rapid prototyping and small-batch manufacturing.

B. Future Work: Cross-Modal Geometry Conditioning

While this work uses multi-view renderings of CAD models as prompts, an important next step is to move beyond rasterized images and explore direct geometric conditioning. Future work could investigate encoding meshes, point clouds, or implicit surface representations directly into the prompt space of foundation models, enabling tighter integration between geometric reasoning and perception, without the middle step of canonical rendering.

REFERENCES

- [1] R. Memmesheimer, J. Nogga, B. Pätzold, E. Krzhkov, S. Bultmann, M. Schreiber, J. Bode, B. Karacora, J. Park, A. Savinykh, and S. Behnke, “Robocup@home 2024 opl winner nimbro: Anthropomorphic service robots using foundation models for perception and planning,” in *Robot World Cup. RoboCup 2024*, ser. Lecture Notes in Computer Science. Springer, 2025, pp. 515–527.
- [2] D. Morrison, A. W. Tow, M. McTaggart, R. Smith, N. Kelly-Boxall, S. Wade-McCue, J. Erskine, R. Grinover, A. Gurman, T. Hunn, D. Lee, A. Milan, T. Pham, G. Rallos, A. Razjigaev, T. Rowntree, K. Vijay, Z. Zhuang, C. Lehnert, I. Reid, P. Corke, and J. Leitner, “Cartman: The low-cost cartesian manipulator that won the amazon robotics challenge,” in *Proceedings of the IEEE International Conference on Robotics and Automation (ICRA)*, 2018.
- [3] N. Carion, L. Gustafson, Y. Hu, S. Debnath, R. Hu, D. Suris, C. Ryali, K. Vasudev Alwala, H. Khedr, A. Huang, J. Lei, T. Ma, B. Guo, A. Kalla, M. Marks, J. Greer, M. Wang, P. Sun, R. Rädle, T. Afouras, E. Mavroudi, K. Xu, T. Wu, Y. Zhou, L. Momeni, R. Hazra, S. Ding, S. Vaze, F. Porcher, F. Li, S. Li, A. Kamath, H. K. Cheng, P. Dollár, N. Ravi, K. Saenko, P. Zhang, and C. Feichtenhofer, “Sam 3: Segment anything with concepts,” *arXiv preprint*, vol. arXiv:2511.16719, 2025. [Online]. Available: <https://arxiv.org/abs/2511.16719>
- [4] X. Peng *et al.*, “Synthesize, diagnose, and optimize: Towards fine-grained vision-language understanding,” in *Proceedings of the IEEE/CVF Conference on Computer Vision and Pattern Recognition (CVPR)*, 2024.
- [5] X. Ju *et al.*, “Evaluation of vision-language models under fine-grained visual discrimination tasks,” *Applied Sciences*, vol. 15, no. 9, 2025.
- [6] Y. Chen, S. Chen, Z.-X. Yang, and E. Wu, “Learning self-target knowledge for few-shot segmentation,” *Pattern Recognition*, vol. 149, p. 110266, 2024.
- [7] A. Kirillov, E. Mintun, N. Ravi *et al.*, “Segment anything,” *arXiv preprint arXiv:2304.02643*, 2023.
- [8] C. Zhang, G. Lin, F. Liu, R. Yao, and C. Shen, “Canet: Class-agnostic segmentation networks with iterative refinement and attentive few-shot learning,” in *Proceedings of the IEEE/CVF Conference on Computer Vision and Pattern Recognition (CVPR)*, 2019, pp. 5217–5226.
- [9] Z. Tian, H. Zhao *et al.*, “Prior guided feature enrichment network for few-shot segmentation,” in *CVPR*, 2020.
- [10] R. Zhang *et al.*, “Personalize segment anything model with one shot,” *arXiv preprint arXiv:2305.03048*, 2023.
- [11] M. Oquab, T. Darcet, T. Moutakanni, H. V. Vo, M. Szafraniec, V. Khalidov, P. Fernandez, D. Haziza, F. Massa, A. El-Nouby, M. Assran, N. Ballas, W. Galuba, R. Howes, P.-Y. Huang, S.-W. Li, I. Misra, M. Rabbat, V. Sharma, G. Synnaeve, H. Xu, H. Jégou, J. Mairal, P. Labatut, A. Joulin, and P. Bojanowski, “Dinov2: Learning robust visual features without supervision,” *arXiv preprint arXiv:2304.07193*, 2023.

- [12] Y. Liu, M. Zhu, H. Li, H. Chen, X. Wang, and C. Shen, "Matcher: Segment anything with one shot using all-purpose feature matching," in *International Conference on Learning Representations (ICLR) 2024*, 2024. [Online]. Available: https://proceedings.iclr.cc/paper_files/paper/2024/hash/4df9a5e6bad9e64ebcea453e031142bb-Abstract-Conference.html
- [13] M. Caron, H. Touvron, I. Misra, H. Jégou, J. Mairal, P. Bojanowski, and A. Joulin, "Emerging properties in self-supervised vision transformers," in *Proceedings of the IEEE/CVF International Conference on Computer Vision (ICCV)*, 2021.
- [14] T.-T. Nguyen, J. Lee, M. Cho, and J. F. Canny, "Cnos: A strong baseline for cad-based novel object segmentation," in *Proceedings of the IEEE/CVF International Conference on Computer Vision Workshops (ICCVW) R6D Workshop*. IEEE/CVF, 2023, p. 338–350. [Online]. Available: https://openaccess.thecvf.com/content/ICCV2023W/R6D/papers/Nguyen_CNOS_A_Strong_Baseline_for_CAD-Based_Novel_Object_Segmentation_ICCVW_2023_paper.pdf
- [15] S. Cho, S. Park, and I. Oh, "Muse: Model-based uncertainty-aware similarity estimation for zero-shot 2d object detection and segmentation," 10 2025.
- [16] X. Li, Q. Zhang, Y. Wang, and K. Chen, "Neural instance detection and segmentation network (nids-net)," *arXiv preprint*, vol. arXiv:2405.17859, 2024. [Online]. Available: <https://arxiv.org/abs/2405.17859>
- [17] H. Su, S. Maji, E. Kalogerakis, and E. Learned-Miller, "Multi-view convolutional neural networks for 3d shape recognition," in *Advances in Neural Information Processing Systems (NeurIPS)*, 2015.
- [18] X. Wei, C. Shen, Y. Wang *et al.*, "View-gcn: View-based graph convolutional network for 3d shape analysis," in *Proceedings of the IEEE/CVF Conference on Computer Vision and Pattern Recognition (CVPR)*, 2019.
- [19] S. Koch, A. Matveev, Z. Jiang, F. Williams, A. Artemov, E. Burnaev, M. Alexa, D. Zorin, and D. Panozzo, "Abc: A big cad model dataset for geometric deep learning," in *Proceedings of the IEEE Conference on Computer Vision and Pattern Recognition (CVPR)*, 2019.
- [20] T. Hodaň, P. Haluza, Š. Obdržálek, J. Matas, M. Lourakis, and X. Zabulis, "T-LESS: An RGB-D dataset for 6d pose estimation of texture-less objects," in *2017 IEEE Winter Conference on Applications of Computer Vision (WACV)*, 2017, pp. 880–888.
- [21] B. Drost, M. Ulrich, P. Bergmann, P. Härtinger, and C. Steger, "Introducing MVTec ITODD — a dataset for 3d object recognition in industry," in *2017 IEEE International Conference on Computer Vision Workshops (ICCVW)*, 2017, pp. 2200–2208.